A widely voltage-tunable quantum cascade laser based on "two-step" coupling

Yu Yao,[1,a] Kale J. Franz,[1] Xiaojun Wang,[2] Jen-Yu Fan,[2] and Claire Gmachl[1]
[1]*Department of Electrical Engineering, Princeton University, Princeton, New Jersey 08544, USA*
[2]*Adtech Optics, Inc., City of Industry, California 91748, USA*

(Received 21 April 2009; accepted 22 June 2009; published online 14 July 2009)

A novel quantum cascade laser design with "two-step" coupling between the injector and the upper laser state is demonstrated to achieve a widely voltage-tunable laser spectrum. Electroluminescence from this design can be tuned over a range of more than 200 cm^{-1} with a tuning coefficient of ~700 cm^{-1}/V per stage. Lasers based on this design provide a tuning range of ~100 cm^{-1} (8.3–9 μm) above threshold with a tuning coefficient of ~900 cm^{-1}/V per stage at a constant temperature of 295 K. © *2009 American Institute of Physics*. [DOI: 10.1063/1.3179165]

The midinfrared (mid-IR) spectral range is of particular interest for applications such as gas analysis and chemical sensing.[1] Quantum cascade (QC) lasers are versatile mid-IR light sources because the wavelength can be designed from 2.7 to 24 μm.[2,3] In many applications, such as detecting multiple trace gases or chemical species with interfering absorption features, a broad wavelength tuning range is required. The prevailing tuning techniques for QC lasers are essentially based on temperature tuning or mechanical tuning. The former has a very limited tuning range (~10 cm^{-1} over the TE cooler temperature range with a tuning rate of ~0.1–0.13 cm^{-1}/K).[2] The latter has a wide tuning range; however, the setup requires well-aligned external components.[4] An alternative way is to tune the laser spectra by simply changing the voltage applied on a QC laser. Widely voltage-tunable intersubband electroluminescence (EL) has been observed in various QC laser designs (the tuning ranges are about 100–200 cm^{-1}) because of the Stark effect in coupled quantum wells.[5] Moreover, to achieve widely tunable single mode QC lasers, a broad gain spectrum is essential.[4,6] Heterogeneous active regions[7] or bound-to-continuum designs[8] can be used to achieve a broad gain spectrum. However, both come at the cost of the peak gain. Voltage tuning of QC laser gain spectra, on the other hand, covers a broad wavelength range without sacrificing the peak gain since it tunes a narrow gain spectrum over a wide range.

In a previous study,[5] we investigated the voltage tunability of the prevailing QC laser designs based on the anticrossed vertical and diagonal transitions as well as the photon-assisted diagonal transition. All designs display voltage-tunable EL. However, lasers based on the anticrossed vertical transition and photon-assisted diagonal transition are not tunable above threshold, while lasers based on an anticrossed diagonal transition active region have a tuning range of about 30 cm^{-1} above threshold at 80 K, much smaller than that of the EL over the same voltage range, which is 60–70 cm^{-1}. The reason of the smaller tuning range for lasers lies in the stimulated emission that drives electrons across the active region.[9] In conventional QC laser designs, most of the electrons accumulate at the lowest injector state and the upper laser state. Below threshold, the electrons transit across the active region mainly via longitudinal-optical (LO) phonon scattering. Above threshold, as the light intensity inside the cavity becomes stronger and stronger, electrons transit across the active region faster and faster via stimulated emission. As a result, the voltage over the active region does not increase as fast any more.

In this letter, we demonstrate a novel QC laser design based on "two-step" coupling between the injector and active region to provide a wide wavelength tuning range for lasers above threshold by simply changing the applied voltage. A portion of the conduction band of this design is shown in Fig. 1. It is based on a two-phonon resonance diagonal transition active region. A coupling state (c) is inserted between the injector ground state (g) and the upper laser state (u). The scattering lifetime (dominated by LO phonon scattering) from the injector states to the coupling state is about 1.5 ps, while the upper laser state scattering lifetime is about 3 ps. In this way, the electron transit across the active region via the stimulated emission above threshold slows down so that the decrease of the differential resistance in the active region is not as fast as the conventional designs when the applied voltage increases. Besides, the coupling state and the upper laser state are strongly coupled, with an energy splitting at resonance of about 11.2 meV. All these features result in a larger

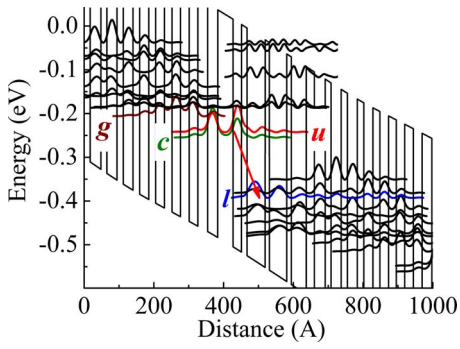

FIG. 1. (Color online) Conduction-band diagram of a portion of the active regions and injectors and the moduli squared of the relevant wave functions of the two-step coupling design under an electric field of 50 kV/cm. The designed emission wavelength is around 8.8 μm at RT. The layer sequence of one period (starting from the injection barrier, in angstrom) is **44**/24/**16**/52/**12** /50/**13**/43/**23**/31/**17**/29/**18/28/19/26/20/25/22/24** **/25/25/28/29, where** $In_{0.52}Al_{0.48}As$ **barrier layers are in bold,** $In_{0.53}Ga_{0.47}As$ **well layers are in normal font, and the underlined layers are doped (Si,** 1×10^{17} cm^{-3}**).**

[a]Electronic mail: yuyao@princeton.edu.

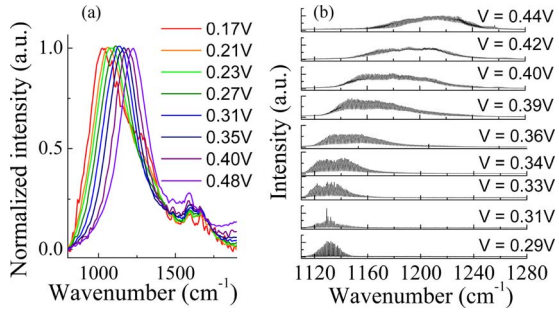

FIG. 2. (Color online) (a) EL from a mesa and (b) spectra of a laser based on the two-step coupling design as functions of the applied voltage per period of active region and injector. All data are taken at $T=295$ K in pulsed mode.

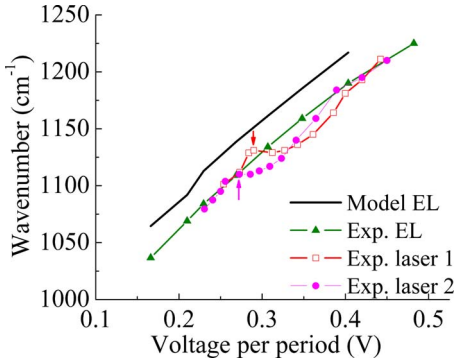

FIG. 3. (Color online) Calculated (solid line) and measured (line+triangles) EL peak wavenumbers from a mesa as well as measured laser emission wavenumbers (line+squares/circles) from laser 1 (1.5 mm cavity length and 12 μm ridge width) and laser 2 (1.5 mm cavity length and 14 μm ridge width) as functions of voltage per period of active region and injector. The arrows indicate the laser thresholds. All experimental results are taken at room temperature ($T=295$ K) in pulsed mode.

dynamic voltage range over the active region above threshold.

The laser was grown by metal-organic chemical vapor deposition on a low-doped InP substrate. The active core includes 37 periods of injector and active region. A 3 μm InP (Si 5×10^{16} cm^{-3}) buffer layer was grown below the active region; 2.6 μm InP (Si 5×10^{16} cm^{-3}) and 1 μm InP (Si 8×10^{18} cm^{-3}) layers were grown above the active core as the upper cladding, followed by a 100 Å thick layer of InP (Si 2×10^{19} cm^{-3}) and a final 100 Å thick layer of InGaAs (Si 5×10^{19} cm^{-3}) as the contact layer.

The wafer was processed into 200 μm diameter circular mesas and deep-etched ridge lasers. The mesas were etched just past the active core with slanted side walls to ensure that the EL would not be impacted by any cavity effect; they were cleaved in half to couple light out. Both conventional ridge lasers (8–15 μm wide) and wide ridge (30 and 60 μm wide) lasers were processed. All lasers have Fabry–Pérot cavities with as-cleaved facets and cavity lengths of 1–3 mm. The wide ridge lasers were also cleaved along the laser ridge to measure the EL emitted from the direction orthogonal to the laser ridge.[10]

EL from the mesas and lasers was measured in pulsed mode (with 100 or 45 ns pulse width, 80 kHz repetition rate) using a Fourier-transform IR spectrometer with a cooled HgCdTe detector. The laser spectra above threshold were also measured under the same conditions. The low duty cycle ensures that the measurement results are not impacted by thermal effects, such as thermal tuning.

Figure 2(a) shows the EL at room temperature (~295 K) from a mesa as a function of voltage per stage. The peak wavenumber of the EL can be determined by fitting the raw data with (if necessary, multiple) Lorentzian peaks.[5] The spectra for a laser from threshold to the power rollover point are shown in [Fig. 2(b)]. To determine the tuning trend of the laser spectra, we measured the wavenumbers on both sides at 10% height of the peak intensity and extracted the midpoint value for the laser wavenumber (the validity of this method will be discussed later). Both the EL peak and laser wavenumbers are shown in Fig. 3, as functions of voltage per stage. The tuning rate of the EL is ~700 cm^{-1}/V, which fits well with the calculated results using a self-consistent Schrödinger–Poisson solver, also shown in Fig. 3. The laser spectra are as tunable as the EL below threshold, followed by a reduced tunability at threshold. The tunability resumes at ~20% above the threshold current density. The tuning rate of the laser spectra above threshold is even higher than that of the EL, about 900 cm^{-1}/V. The total tuning range of lasers above threshold is about 80–100 cm^{-1}, which is as wide as that of the EL over the same voltage range above laser threshold.

In order to compare the laser wavenumbers obtained by the method mentioned above with the peak wavenumbers of the laser gain spectra, we measured the EL from the direction orthogonal to the laser ridge[10] below and above threshold. A typical EL measured from such a laser above threshold is shown in the inset of Fig. 4. The narrow emission peak is because of the scattered stimulated emission from defects inside the laser cavity. To obtain the EL peak, the laser emission peak is removed and the rest of the data are fitted with multiple Lorentzians. The peak wavenumber of the gain spectrum is determined by the peak of the fitted curve. The gain spectra peak and laser wavenumbers (obtained from laser spectra by the method mentioned above) for a typical laser are compared in Fig. 4, as a function of injection current. One can see that they display almost the same wavenumbers and tuning behavior.

From the tuning behavior of the laser spectra, we can conclude that this design has a much earlier resumed tunability than the conventional anticrossed diagonal designs.[5] As mentioned earlier, the reason lies in the two-step injection scheme. The lasers still see a drop of differential resistance at

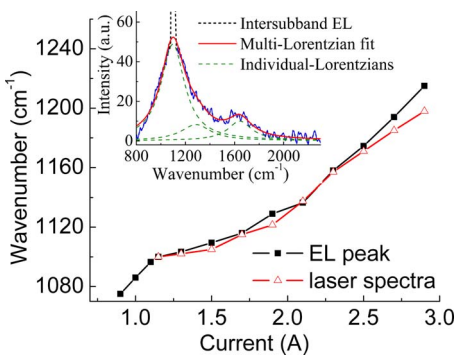

FIG. 4. (Color online) EL peak wavenumbers and laser emission wavenumbers measured from the direction orthogonal to the laser ridge. All experimental data were measured at room temperature (~295 K) in pulsed mode (80 kHz, 45 ns pulse width). The figure inset shows the intersubband EL detected from a laser 20% above threshold and the fitted curve.

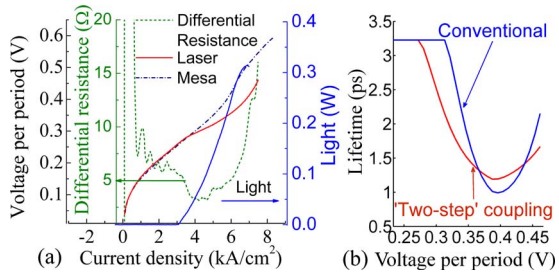

FIG. 5. (Color online) (a) Measured voltage and light versus current density (*LJV*) characteristics and differential resistance of a laser as well as *JV* characteristics of a mesa. All data were measured at $T=295$ K in pulsed mode. (b) Calculated effective upper laser state lifetime as a function of applied voltage for the two-step coupling design and a comparable conventional laser design.

threshold, as shown in [Fig. 5(a)], indicating a dramatic decrease of the upper laser state lifetime (τ_u, including the scattering lifetime and stimulated emission lifetime) because of the stimulated emission. However, as τ_u decreases until it is shorter than the scattering lifetime between the injector states and the coupling state, more electrons will accumulate in the injectors and less electrons in the upper laser state and the coupling state. As a result, the light intensity is not increased as fast as the applied voltage increases; therefore the drop of τ_u and the differential resistance over the active region slows down. This can be verified by the calculated results of τ_u using a rate equation model for the two-step coupling design and a conventional design with parameters obtained from the Schrödinger–Poisson solver,[11] as shown in [Fig. 5(b)]. The slow down of the decrease of the upper laser state lifetime and the electron accumulation in the injectors leads to a higher voltage increase over the active region but a lower voltage increase over the injectors. Moreover, this design has a larger dynamic voltage range compared with the conventional anticrossed diagonal designs, as one can see from the light-voltage-current density characteristics shown in [Fig. 5(a)]. The voltage range from the laser threshold to rollover point is almost 30% of the applied voltage at threshold, compared with less than 10% for conventional designs.[5] Simply stated, a larger voltage dynamic range and larger voltage increase over the active region contribute to a wider voltage-induced wavelength tuning range, i.e., $\sim 100\ \mathrm{cm}^{-1}$.

The performance of QC lasers is always a key issue in real world applications. Lasers based on the two-step coupling design have comparable output power (more than 1.4 W double-facet output from a 3 mm long, 15 μm wide ridge laser) and slope efficiency (~ 1 W/A) as well as temperature performance ($T_0=170$ K) with the best reported QC lasers at similar wavelengths.[12] However, they show a higher threshold current density ($\sim 3.5\ \mathrm{kA/cm}^2$ at $T=295$ K). We attribute this to an early turn-on voltage and concomitant leakage current because of the electron transition from the coupling state to the lower states in the active region before achieving the strong tunneling between the coupling state and the injector states. Further improvement on the structure will optimize the gain for a lower applied voltage and reduce the doping density.

In conclusion, we have demonstrated a QC laser design based on two-step coupling to achieve widely voltage-tunable QC lasers. Electroluminescence from this design has a tuning range over 200 cm^{-1}; lasers based on this design can be tuned over $\sim 100\ \mathrm{cm}^{-1}$ above threshold at a constant temperature $T=295$ K, which is about a threefold increase compared with earlier designs.

This work is supported in part by MIRTHE (NSF-ERC Grant No. EEC-0540832).

[1] A. A. Kosterev and F. K. Tittel, IEEE J. Quantum Electron. **38**, 582 (2002).
[2] C. Gmachl, F. Capasso, D. L. Sivco, and A. Y. Cho, Rep. Prog. Phys. **64**, 1533 (2001).
[3] R. Teissier, J. Devenson, O. Cathabard, and A. N. Baranov, Conference on Lasers and Electro-optics, San Jose, CA, May 4–9 2008, (unpublished).
[4] R. Maulini, M. Beck, J. Faist, and E. Gini, Appl. Phys. Lett. **84**, 1659 (2004).
[5] Y. Yao, Z. Liu, A. J. Hoffman, K. J. Franz, and C. F. Gmachl, IEEE J. Quantum Electron. **45**, 730 (2009).
[6] B. G. Lee, M. A. Belkin, R. Audet, J. MacArthur, L. Diehl, C. Pflügl, and F. Capasso, Appl. Phys. Lett. **91**, 231101 (2007).
[7] C. Gmachl, D. L. Sivco, R. Colombelli, F. Capasso, and A. Y. Cho, Nature (London) **415**, 883 (2002).
[8] J. Faist, M. Beck, and T. Aellen, Appl. Phys. Lett. **78**, 147 (2001).
[9] H. Choi, L. Diehl, Z. Wu, M. Giovannini, J. Faist, F. Capasso, and T. B. Norris, Phys. Rev. Lett. **100**, 167401 (2008).
[10] R. Colombelli, F. Capasso, C. Gmachl, A. Tredicucci, A. M. Sergent, A. L. Hutchinson, D. L. Sivco, and A. Y. Cho, Appl. Phys. Lett. **77**, 3893 (2000).
[11] Y. Yao, K. J. Franz, Z. Liu, A. J. Hoffman, and C. F. Gmachl, Proceedings of the SPIE, 2009 (unpublished).
[12] Q. Wang, C. Pflüg, L. Diel, F. Capasso, T. Edamura, S. Furuta, M. Yamanishi, and H. Kan, Appl. Phys. Lett. **94**, 011103 (2009).